



1 **Knickpoints and Fixpoints: The Evolution of Fluvial Morphology**
2 **under the Combined Effect of Fault Uplift and Dam Obstruction on a**
3 **Soft Bedrock River**

4 Hung-En Chen¹, Yen-Yu Chiu¹, Chih-Yuan Cheng¹ and Su-Chin Chen^{1,2}

5 ¹ Department of Soil and Water Conservation, National Chung Hsing University, Taichung 40227, Taiwan

6 ² Innovation and Development Center of Sustainable Agriculture, National Chung Hsing University, Taichung 40227, Taiwan

7 *Correspondence to:* Su-Chin Chen (scchen@nchu.edu.tw)

8 **Abstract.** Rapid changes in river geomorphology can occur after being disturbed by external factors like earthquakes or large
9 dam obstructions. Studies documenting the evolution of river morphology under such conditions have advanced our
10 understanding of fluvial geomorphology. The Dajia River in Taiwan presents a unique example of the combined effects of a
11 coseismic fault (the 1999 Mw 7.6 Chi-Chi earthquake) and a dam. As a result of the steep terrain and abundant precipitation,
12 rivers in Taiwan have exhibited characteristic post-disturbance evolution over 20 years. This study also considers two other
13 comparative rivers with similar congenital conditions: the Daan River was affected by a thrust fault Chi-Chi earthquake, too;
14 the Zhuoshui River was influenced by dam construction finished in 2001. The survey data and knickpoint migration model
15 were used to analyze the evolution of the three rivers and propose hypothesis models. Results showed that the mobile
16 knickpoint migrated upstream under the influence of flow, while the dam acted as a fixpoint, leading to an increased elevation
17 gap and downstream channel incision. Thereby, the Dajia river narrowing and incision began at both ends and progressively
18 spread to the whole reach under the combined effects.

19 **KEYWORDS:** dam obstruction; fixpoint; coseismic uplift; knickpoint; soft bedrock incision; river evolution



20 1. Introduction

21 Natural tectonic movements and artificial structures are the main factors that disturb river equilibrium. These external
22 influences often interact complexly; therefore, distinguishing between anthropogenic and natural drivers of landscape
23 evolution is difficult. In addition, changes in these external conditions, in turn drive adjustments in the riverbed, generating
24 new landscape patterns. River morphological development generally reflects the geology and flow stress conditions (Lyell,
25 1830). When a significant external impact occurs, a knickpoint (a localized discontinuity in the longitudinal profile of the
26 riverbed) often forms (Holland, 1976). Knickpoints can range in scale from a single waterfall to a zone of several kilometers
27 (Crosby and Whipple, 2006) and may result from natural factors such as extreme weather, sea-level fall, and earthquake-
28 induced surface rupture (Seidl and Dietrich, 1992; Whipple, 2004, Bishop et al., 2005; Heijnen et al., 2020).

29 The active fault causes a prominent knickpoint in stream, known as tectonic uplift, leading to a local increase in channel
30 steepness (Hayakawa et al., 2009; Huang et al., 2013; Cook et al., 2013). The sudden elevation change in the riverbed divides
31 the river profile into two reaches with differing slopes, altering the base level of fluvial erosion. The increasing flow stress
32 erodes the knickpoints, causing it to migrate upstream-ward over time. A long duration is required for the fluvial response to
33 adapt to localized surface uplift or depositional blockage by knickpoint retreat and migration upstream with time, cutting a
34 narrow channel and even forming a canyon. The migration process and speed are highly variable and depend on the tectonic
35 setting and physical nature of the riverbed (Whipple et al., 2004). The emergence and migration of knickpoints caused by
36 disturbance from external conditions was studied extensively (Whipple, 2001; Whipple and Trucker, 2002; Crosby and
37 Whipple, 2006; Clark, 2014; Ahmed et al., 2018).

38 Anthropogenic factors, such as reservoir construction, which is one of the most common ways humans interfere with river
39 hydrology and sedimentation (Magilligan and Nislow, 2005; Petts and Gurnell, 2005; Graf, 2006; Nelson et al., 2013; Liro,
40 2017, 2019; Zhou et al., 2018). Dam as a fixpoint in the river influences two critical components of river geomorphology: the
41 sediment transport capacity of the flow and the oncoming sediment load (Williams and Wolman, 1984). If the sediment
42 transport capacity exceeds the oncoming sediment load, the amount of sediment may be insufficient to maintain the riverbed
43 level, and erosion may occur. Conversely, if the sediment load exceeds the sediment transport capacity, deposition on the
44 riverbed would be expected to occur. The self-adjustment mechanisms of river channels responding to insufficient or excess
45 sediment (Brandt, 2000) results in the change in cross-section geometry, bed material size, river pattern, and slope. Previous
46 studies on the evolution of areas downstream of dams have primarily analyzed changes in downstream sandbars over large



47 spatial scales (Horn et al., 2012; Słowik et al., 2018; Kong et al., 2020) or the ecology of the lower reaches in front of dams
48 (Kingsford, 2000; Braatne et al., 2008; Shafroth et al., 2016). There have been few studies of exposed bedrock based on long-
49 term observations (Inbar, 1990). In most cases, a dam effectively traps the sediment supply from the watershed. If sediment
50 transfer to the downstream reaches of the dam is reduced, the armor layers of the riverbed are lost, which may cause an incision
51 of the fluvial channel (Surian and Rindai, 2003). This incision subsequently narrows the river cross-sections and lowers the
52 thalweg level.

53 Decades or hundreds of years are generally required for a riverbed to reach a new equilibrium after disturbance by external
54 conditions, so it is difficult to understand such changes based on short-period observational data (Howard et al., 1994; Tomkin
55 et al., 2003). Because of the abundant rainfall brought by typhoons and monsoons, the river terrain in Taiwan can alter
56 dramatically over a short period of time. Moreover, dams in Taiwan are built primarily in steep reaches, enhancing the rapid,
57 remarkable morphological evolution of the downstream reaches. The reservoirs of dams constructed on the rivers become
58 silted up, resulting in a lack of sediment downstream in the meantime, which causes loss of armor layers, exposure of soft rock,
59 and severe erosion. Another factor influencing the distinctive characteristics of Taiwanese rivers is the geological location;
60 Taiwan is located in a plate junction zone that experiences frequent earthquakes such as the Chi-Chi Earthquake of 1999 (Lin
61 et al., 2001; Ota et al., 2005), which caused the offset of Chelungpu thrust fault in central Taiwan. The surface rupture and
62 uplift induced the formation of knickpoints and river gorges. Twenty years later, the undercutting trend of the active channel
63 below dams and the migration of post-earthquake knickpoints have caused the rivers to evolve into their present forms. This
64 rapid evolution of river morphology over a short time makes Taiwan rivers suitable as case studies. The Dajia River is a unique
65 example, as a dam structure and coseismic uplift impact it simultaneously in a short reach. The current work aims to clarify
66 the river changes caused by the earthquake and a dam, and to propose a hypothesis for the evolution model. To compare the
67 various morphological developments under different external conditions, the Daan, Zhuoshui, and Dajia rivers in central
68 Taiwan are considered in this study.

69 2. Study area, materials, and methods

70 The longitudinal changes of the river bed and the accompanying river pattern changes are the objects of observation. A
71 common type of longitudinal profile development for knickpoint retreat is illustrated in Fig. 1a (Gardner 1983; Whipple and
72 Trucker, 1999; Parker and Izumi 2000; Alonso et al. 2002; Bressan et al., 2014). As the base level of erosion fell and the abrupt
73 slope caused acceleration of the flow, the stream eroded the bed. During this process, apparent upstream degradation and



74 downstream aggradation occurred. The knickpoint migrated upward with time, accompanying by slope replacement. After the
75 river had reached a new equilibrium in a channelized pattern, the slope replacement resulted in a natural profile. During the
76 adjustment, the incision trend gradually slowed, and sedimentation may commence downstream (dashed line in Fig. 1a). The
77 profile evolved from a concave curve to a graded profile (Chamberlin and Salisbury, 1904). The well-known result of dam
78 construction is the progressive loss of the armor layer in the neighboring downstream river (Fig. 1b). The scouring baseline
79 extended downstream-ward from the dam (Olsen, 1999; Choi et al., 2005; Słowik et al., 2018). Because of the fixpoint, the
80 local slope at the dam toe became steeper progressively, and the dam caused the downstream river profile to be gentle and
81 sediment transport to decrease.

82 However, significant changes in the longitudinal profile must also be accompanied by variations in river patterns, which
83 have yet to receive much attention. Furthermore, the interaction between fault scarps and dam obstructions within a river reach
84 is rarely observed and studied. To address these gaps, we collected historical data for three rivers in Taiwan (Daan, Zhuoshui,
85 and Dajia), each representing the individual effects of faults and dams, as well as their combined effects.

86 2.1 Study area

87 Taiwan's climate is strongly affected by the western Pacific tropical cyclone. There are approximately three to four
88 typhoons and heavy rain events yearly, and the average annual precipitation is about 2500 mm. The heavy rains during the
89 monsoons and typhoons cause dramatic changes to riverbeds over short periods of time. In addition, because Taiwan is located
90 at the compressive tectonic boundary between the Eurasian and Philippine Sea plates, the collision of the two continental plates
91 causes tectonic breakage of the strata. On September 21, 1999, the Chi-Chi earthquake ($M_w = 7.6$) resulted in uneven uplift in
92 the island. Three central Taiwan rivers illustrate dams or faults' effects (Figure 2): The Daan River has been affected by vertical
93 fault scarps, the Dajia River by both fault scarps and a dam, and the Zhuoshui River by dam obstruction. These three important
94 rivers have very similar characteristics: their east-to-west flow direction; their range of elevation from sea level to ~3000 m;
95 their steep river slopes (the average slopes of the middle and upper reaches are greater than 1/60); and the presence of soft
96 rock in the mid-stream (as shown in the pink region in Figure 2). The locations of the three rivers and the Chelungpu thrust
97 fault are marked in Figure 2. The southern termination of the fault crosses the Zhoushui River trending north-south; the
98 northern termination near the Dajia and the Daan rivers shows a complex deformation pattern trending NE-SW to E-W (Lee
99 et al., 2002), composed of several parallel thrust faults. In the three studied reaches, the Pleistocene sedimentary rocks are
100 mainly composed of soft rocks consisting of sandstone, siltstone, shale, and mudstone. These rocks are generally poorly



101 lithified and weakened by a high water content; therefore, their resistance to water erosion is poor. The riverbed rock is readily
102 incised by flooding flow when the upper armoring protective layer was lost (Huang, 2014).

103 The Chi-Chi earthquake produced a surface rupture 80 km long (Lee et al., 2002). Several fracture planes at the north
104 end of the fault caused uneven uplift in the region. One of the ruptures passed through the right bank of the Shigang Dam on
105 the Dajia River, causing serious damage to the dam structure. The maximum vertical displacement of the surface rupture was
106 9 m, increasing the drop height of the bed level between the face and the back of the dam markedly. The repaired Shigang
107 Dam was intended to store $2.4 \times 10^6 \text{ m}^3$ of water after the Chi-Chi earthquake; however, owing to deposition in the reservoir,
108 only $\sim 1.4 \times 10^6 \text{ m}^3$ of water can now be retained. The original armor layers on the riverbed in front of the Shigang Dam were
109 lost rapidly, and the soft bedrock was exposed. The two rupture surfaces at the north end of the Chelungpu Fault uplifted a 1
110 km reach of bed in the Daan River, with a maximum vertical uplift of 10 m.

111 Although the southern end of the Chelungpu Fault passes downstream of the Jiji Dam (Zhuoshui River), the fault uplifted
112 the bed level by ~ 2 m, less than the uplifts in the Daan and Dajia rivers. The Jiji Dam was built in 2001 (after the 1999 Chi-
113 Chi earthquake), is situated on the narrowest part of the Zhuoshui River, and has a maximum designed storage capacity of 10
114 $\times 10^6 \text{ m}^3$. Due to the large sediment yield in the Zhuoshui River watershed, the present-day adequate water storage capacity is
115 only $\sim 4 \times 10^6 \text{ m}^3$. The Jiji Dam downstream is known for its soft bedrock canyon features, formed by dam-obstructed water
116 scouring.

117 2.2 Materials

118 Analysis of the effects of faults and dams, alteration of river patterns, changes in thalweg levels, and variations in river
119 cross-sections are crucial to revealing the process of river evolution. SPOT-5 and SPOT-6 satellite images and orthographic
120 images obtained by the Center for Space and Remote Sensing Research, National Central University (CSRSR/NCU) and Aerial
121 Survey Office (AFASI) of Taiwan were used to assess changes in river patterns. Multiyear cross-sectional and longitudinal
122 profiles were established from historical surveys by the Water Resources Agency (WRA). Additional analyses of knickpoint
123 retreat and variations in river elevation and width were carried out. The locations of knickpoints were determined by identifying
124 abrupt terrain changes and the positions of splash in the images. In order to analyze the variation of channel width (W), depth
125 (D), and aspect ratio (W/D), we calculated the bank-full discharge width and depth, which represents the maximum flow that
126 can occur in a river before water starts overflowing and spreading out onto the floodplain. We identified the river banks and
127 extracted channel widths from orthographic images. The banks were defined as the boundaries between the main channel and



128 the adjacent floodplain.

129 2.3 Mathematical model

130 The application of the mathematical model provides an abstract description of a concrete system using physical concepts
131 and mathematical language. A one-dimensional Exner equation (Exner, 1925) is used to describe the advective and diffusive
132 knickpoint migration (Bressan et al., 2014):

$$133 \quad \frac{\partial z}{\partial t} + \frac{1}{(1-p_s)} \frac{\partial q_s}{\partial x} = 0 \quad (1a)$$

134 where z is the bed elevation along the thalweg, p_s is the porosity of bed sediment, t is the time, x is the distance, and q_s is
135 the sediment discharge per unit width that is estimated by the product of the surface height change η , and the knickpoint
136 migration rate dx/dt is expressed as equation 1b.

$$137 \quad q_s = -\eta \frac{dx}{dt} \quad (1b)$$

138 The migration rate as a sediment separation per unit area homogeneously distributed over the eroding surface is expressed
139 as equation (1c).

$$140 \quad \frac{dx}{dt} = k_d [\tau(x) - \tau_c] \quad (1c)$$

141 where k_d is the erodibility, τ is the bed shear stress, and τ_c is the critical shear stress of the bed material. The condition of
142 an obvious knickpoint face, τ should be estimated using a formula that considers knickpoint as a submerged obstacle
143 (equation (1d)) (Engelund, 1970).

$$144 \quad \tau(x) = M\tau_0 \left[1 + A \frac{(z-z_0)}{H_0} + B \frac{\partial z}{\partial x} \right] \quad (1d)$$

145 The factors M , A , and B in equation (1d) are parameters related to localized phenomena. τ_0 , z_0 , and H_0 are the shear
146 stress, bed elevation and the water depth upstream of the knickpoint. The term $B \frac{\partial z}{\partial x}$ represents the change in shear stress due
147 to the local slope. The shear stress in the channel section upstream of the knickpoint crest ($\tau_0 = \gamma H_0 S_0$, where γ is the specific
148 weight of water changes across the knickpoint due to the abrupt change in bed topography (equation (1d)). Substituting
149 equations (1b)–(1d) into equation (1a), equations (2a)–(2c) were obtained in below:

$$150 \quad \frac{\partial z}{\partial t} - C \frac{\partial z}{\partial x} - D \frac{\partial^2 z}{\partial x^2} = 0 \quad (2a)$$

$$151 \quad C = \left(\frac{\eta k_d \gamma}{1-p_s} \right) S_0 M A \quad (2b)$$

$$152 \quad D = \left(\frac{\eta k_d \gamma}{1-p_s} \right) S_0 H_0 M B \quad (2c)$$

153 where the coefficients of the first- and second-order spatial derivatives, C and D , are known as the advection and diffusion



154 coefficients, respectively. It can be concluded that the key controls of the knickpoint retreat are the channel slope, the erodibility
155 of the bed of the river reach, the knickpoint face height, and the upstream water depth. Therefore, the present equation is a
156 physical-based model that can be solved with the second-order accurate implicit finite difference scheme which was
157 implemented in MATLAB.

158 3. RESULTS

159 3.1 Fault effect on Daan River canyon

160 The scarps across the Daan River that were uplifted by the Chi-Chi earthquake caused a dramatic change in the topography,
161 disturbing the dynamic equilibrium of the fluvial system. Cook et al. (2013) proposed that the knickpoint propagated rapidly
162 after 2004 and pointed out that, after the disappearance of bedload, the tool effect caused pronounced fluvial incision of the
163 bedrock. Knickpoint propagation was influenced by the antiformal geological structure of the area, the presence and orientation
164 of interbedded strong and weak lithologies, and the proportion of discharge entering the main channel. Huang et al. (2013)
165 also proposed that the knickpoint retreat rate can be affected by several factors, including discharge, rock properties, geological
166 structures, and bedrock orientation. The channel development of the studied reach and the behavior of knickpoint retreat were
167 assessed by analyzing multiyear data on the form and cross-section of the river.

168 Successive orthographic images of the studied reach of the Daan River from 2000 to 2017 and the corresponding flow
169 paths are illustrated in Fig. 3. River cross-sections constructed from precise survey data are provided in Fig. 4. Chronological
170 longitudinal profiles of the river reach are shown in Fig. 5. Longitudinal profile data from Cook et al. (2013) were included to
171 make information more complete. The effect of the earthquake on the surface elevation is clearly visible in Fig. 5. In addition
172 to the survey data, the advective and diffusive knickpoint migration model (equation 2) was solved to mathematize the
173 knickpoint retreat progress after Chi-Chi earthquake. The initial condition and boundaries condition are needed to solve the
174 equation. The initial condition is the longitudinal profile in 1999, while the boundary conditions are the real bed changes in
175 upstream and downstream boundaries. The C and D are physical parameters and were calibrated by the survey data. In equation
176 2, C represents the moving speed, and D represents the diffusion constant. These two coefficients reflect the rate of bed erosion,
177 which is physically composed mainly of bed shear stress (equations 2b and 2c). Due to the actual bed erosion rates varying
178 with time, the parameters were adjusted to match the real changes. Before 2004, C was 22.0 m/yr, and D was 10.0 m²/yr; after
179 2004, C was 91.5 m/yr, and D was 18.5 m²/yr, and the simulation was continued until 2011 when the knickpoint disappear.
180 The result of the modeling is shown at the top left corner in Fig. 5. The knickpoint progressively retreats, accompanying by slope



181 replacement. The variation trend of the simulation and survey data is generally consistent, and the speed (C) has a larger value
182 in 2004–2011, which is also consistent with the observation.

183 The long-term development of the studied reach of the Daan River in the past 20 years, after the coseismic uplift, can be
184 divided into three periods: downstream erosion and slow knickpoint migration (earthquake to 2004); sudden migration of the
185 knickpoint (2004–2011); and gorge widening and eradication (2011–present).

186 **3.1.1 Downstream erosion and slow knickpoint migration (earthquake to 2004)**

187 After the Chi-Chi earthquake, coseismic ground deformation created a pop-up obstruction across the river, forming a
188 barrier lake behind the rupture scarp. The obstacle blocked the river flow and trapped the sediment, causing the river bed
189 downstream of the rupture scarp completely lose the armor layer. When the armor layer was lost, bedrock incision occurred
190 downstream of the uplifted zone, and the knickpoint retreat appeared. On the other hand, no significant erosion occurred
191 between cross-sections **a** and **b** during that period (Figs 3 and 4). A comparison of the cross-sections for 2000 and 2004 (Fig.
192 4) reveals that most parts of the section **a** even experienced deposition. Slight erosion in some places can be detected in the
193 longitudinal profiles (Fig. 5) between 1999 (after the earthquake) and 2004. Although the seismic uplift produced an obvious
194 knickpoint on the riverbed, that knickpoint migrated only slightly (85 m; Table 1) between 2000 and 2004. The downstream
195 reach of the uplifted zone showed evidence of scour, but no noticeable bedrock incision or canyon landscape had developed
196 yet.

197 **3.1.2 Sudden migration of knickpoint (2004–2011)**

198 The orthographic image for 2007 (Fig. 3) clearly shows that the armor layer had been removed, the bedrock had been
199 exposed, and the deep incision had formed a narrow channel. The knickpoint retreated upstream-ward by approximately 422
200 m between 2004 and 2007, accompanied by continued scouring downstream. In the uplifted reach, under the stress of the
201 concentrated flow in the newly formed channel, the tool effect resulted in a deepened incision of the rock bed, and a canyon
202 landform gradually developed. In the 2007 cross-section data for section **a**, a canyon close to the left bank can be observed,
203 which persisted until 2011. A rapid incision rate (5.6 m/yr) occurred in section **a**, which also experienced a narrowing rate of
204 about 105.5 m/yr. Bed incision and narrowing of the main channel occurred in section **b** simultaneously, with a narrowing rate
205 of approximately 89.9 m/yr and an incision rate of about 2.1 m/yr. Between 2007 and 2011, the knickpoint retreated upstream
206 by about 412 m; the incision at section **a** was lessened, but section **b** experienced a notable incision into the rock bed
207 accompanied by knickpoint retreat. Because an obvious gorge channel had appeared in the uplifted zone, sediment from



208 upstream was transported downstream, and downstream scouring transformed gradually into sedimentation; therefore, the
209 convex longitudinal profile was gradually erased.

210 3.1.3 Gorge widening and eradication (2011 to the present)

211 After 2011, the knickpoint became insignificant in the longitudinal profile, so the thalweg scouring trend slowed. The
212 morphology development is dominated by lateral erosion instead of vertical incision. The narrow, deep canyon evolved into a
213 U-shaped canyon with a wide bottom. River pattern migration from upstream caused the canyon-type channel to commence
214 transforming into a braided channel. The main channel of section **a** experienced deposition as a result of the sediment supply
215 being adequate (Fig. 5). Cook et al. (2014) proposed a mechanism of gorge eradication, called *downstream sweep erosion*,
216 which rapidly transformed the gorge into a beveled floodplain through the downstream propagation of a wide erosion front
217 located where the broad upstream channel abruptly became a narrow gorge. The sweep boundary is clearly visible in the
218 orthographic images for 2011 and 2017 (Fig. 3). Additional large floods are expected to cause a marked widening of the channel
219 instead of deepening (Huang et al., 2013). It has been estimated that removal of the gorge erosion will take 50 years (Cook et
220 al., 2014).

221 Significant incision of the channel is common after a riverbed has been uplifted suddenly by topographic tectonic
222 movement and the bed slope changes dramatically (Merritts et al., 1989). This was the case for the Daan River after the Chi-
223 Chi earthquake. After the coseismic uplift, the base level of erosion downstream reduced, so erosion increased. The river width
224 became notably narrower and deeper. Upward movement of the knickpoint caused the river channel in the uplifted section to
225 narrow rapidly. The concentrated flow caused a rapid incision of a weak geological layer in the riverbed, so the channel width
226 decreased sharply. Therefore, the uplifted section formed a canyon landform. As the slope at the knickpoint gradually recovered,
227 the incision slowed and sediment transport down the recovered river resulted in sediment deposition in the downstream channel.
228 The river also gradually developed lateral erosion upstream, and the river channel tended to widen. The channelization is
229 expected to have been swept because the sweep boundary migrated progressively downward.

230 3.2 Jiji Dam effect on Zhoushui River

231 Construction of the Jiji Dam on the Zhoushui River began in 1996 and operated in 2001. Orthographic images, flow paths
232 of the studied reach, and the locations of cross-sections **c**, **d**, and **e** below the Jiji Dam for 1998 to 2018 are provided in Fig. 6.
233 Chronological survey data of cross-sections **c**, **d**, and **e** are provided in Fig. 7. Chronological longitudinal profiles of the studied
234 reach are illustrated in Fig. 8. The river is located at the southern termination of the Chelungpu Fault (Fig. 1), where the



235 elevation gap caused by the earthquake is relatively small. In 1998, the Zhoushui River was a broad braided river, with many
236 sandbars downstream of the dam (Fig. 6). In 2003, two years after dam operation had commenced, the riverbed armor layer
237 had been lost and the exposed soft bedrock was clearly visible within 700 m of the toe of the dam, because of a lack of sediment.
238 From 2003 to 2007, the effect zone gradually expanded, and exposed bedrock extended to ~3.2 km downstream from the dam.
239 The bedrock's incision deepened due to the tool effect, and the flow path concentrated gradually in front of the dam. Between
240 2007 and 2018, the channelization and the zone with exposed bedrock expanded continuously to 6.5 km downstream of the
241 dam. Due to the channelization, the river cross-section became narrow and deep.

242 The transformation of the river and the rates of lateral and vertical change are clearly visible in the river cross-sections
243 (Fig. 7). There was no apparent erosion of section **c** in 2008, but the sections closer to the dam (**d** and **e**) exhibited obvious
244 incision (Fig. 7). After the loss of the riverbed armor layer, the flow cut down into weak bedrock. The deep main channels'
245 development is clearly visible in sections **d** and **e** between 1998 and 2008. During this time, the incision rate of section **e** was
246 around 1.2 m/yr, and the narrowing rate was around 25 m/yr. During 2008–2012, engineering measures were installed:
247 groundfills were added to the river channel to prevent erosion, and the riverbed level rose slightly at section **e**. However, the
248 channel width of section **c** was markedly narrower, with a narrowing rate of roughly 65 m/yr. Between 2008 and 2015, the
249 incision rates of sections **c** and **d** were roughly 1.4 m/yr. Stratified erosion is apparent in the chronological longitudinal profiles
250 (Fig. 8). Incision of the studied reach became increasingly severe: incision commenced at section **e** and subsequently extended
251 downstream to sections **d** and **c**. We infer that headward erosion did not dominate the riverbed because the Chelungpu Fault
252 passed through the river some distance from the dam and caused only 2 m of uplift; on the contrary, dam-induced downward
253 incision of the riverbed caused degradation of the reach. There is an approximately 15 m difference between the bed level of
254 1998 and that of 2018.

255 The studied reach of the Zhoushui River was a braided river prior to building of the dam. After dam construction, sediment
256 transport was restricted, causing loss of the armor layer downstream under the influence of the tool effect, a deeply incised
257 channel formed in the weak soft bedrock in front of the dam. The flow gradually became concentrated in the deep channel, the
258 river width decreased markedly, and the effect continued to extend downstream with time.

259 3.3 The combined effect of Shigang Dam and Fault on Dajia River

260 The studied reach of the Dajia River, which lies downstream of the Shigang Dam, was affected by both the dam and uplift
261 caused by the Chi-Chi earthquake. The Shigang Dam was broken by uneven uplift of the fault scarp across the dam (9 m on



262 the right side and 3 m on the left), and the downstream section **f** rose by ~7 m (see Fig. 2). The earliest knickpoint formed close
263 to section **f**. The base level of erosion declined downstream after uplift causing the knickpoint to move headward. During
264 2000–2005, the knickpoint retreated by ~400 m, and another new knickpoint formed between sections **g** and **h** (Fig. 9). The
265 damming effect of the Shigang Dam also caused the armor layer to be removed. The bedrock became exposed shortly after the
266 earthquake; however, section **f** was obviously incised during 2000–2005, whereas incision of section **g** did not occur until
267 2005–2008 (Fig. 10). Between 2000 and 2005, engineering measures were installed on several occasions to mitigate the
268 obvious erosion. Groundsills and energy-dissipation measures were constructed in front of the dam; as a result, the flow path
269 between section **g** and the dam became a floodplain.

270 The incision rate of section **g** was ~1.1 m/yr during 2005–2008, and the narrowing rate was ~47.7 m/yr. During the same
271 time interval, the downstream knickpoint (between sections **f** and **g**) disappeared due to river training in 2008. The knickpoint
272 between section **g** and section **h** retreated rapidly toward the dam (Figs 9, 11). During 2005–2008 and 2008–2017, the
273 knickpoint moved upstream by approximately 186 and 219 m, respectively. This retreat of the knickpoint implies that river
274 channel scouring did not stop. Because the riverbed strata trend northeast–southwest, flow scouring preferentially deepened
275 the left part of the rock bed, which moved the channel closer to the left bank. After 2008, the flow channel extended closer to
276 the toe of the dam. Due to the severe incision, the government started surveying section **h** after 2010 (Fig. 10). Significant
277 bedrock incision was recorded, with an incision rate of ~1.4 m/yr at section **h** during 2010–2017. The channel starting from
278 the toe of the dam was not connected with the channel caused by headward erosion from section **f** (Fig. 9) until 2017. The
279 2017 photograph shows a single, meandering channel that starts from the dam and runs through sections **h** and **g**, eventually
280 reaching section **f**, where the knickpoint had initially formed (Fig. 10). Overall, the area downstream of the Shigang Dam
281 displayed headward erosion of the knickpoint and incision of the rock bed in front of the dam.

282 In the Dajia River, the advection and diffusion equation (equation 2) was also used to represent the variation mode of
283 knickpoint and bed elevation. The initial condition is the longitudinal profile in 2000. The coefficients C and D were influenced
284 by bed shear stress. Due to the rapid increase in actual bed erosion rate after 2005, the parameters were adjusted to match the
285 actual changes. Before 2005, C was 7.5 m/yr, and D was 1.825 m²/yr; after 2005, C was 36.5 m/yr, and D was 9.125 m²/yr, and
286 the simulation was continued until 2017. The downstream boundary adopts the real bed change, while the upstream boundary
287 condition is fixed, considering the dam is a fixed point. The bed is progressively scoured in the nearby downstream of the dam,
288 and the knickpoint retreats and gradually fades away. The variation trend of the simulation and survey is generally consistent,



289 excluding the fact that intensive engineering works have been conducted in front of the dam to stabilize the bed.

290 4. Discussion

291 Data on the changes in the riverbed, river width, and migration distance of the knickpoint for all three studied reaches are
292 provided in Table 1. Also, in Fig. 12(a), We use “T” symbols to represent the channel width (W) and depth (D) of the cross-
293 sections in three study reaches, and the aspect ratio (W/D) is labeled above every “T.” After the Chi-Chi earthquake, the
294 channel geometry was not disturbed immediately, and the aspect ratio of the Daan River exhibited only slight changes.
295 Consequently, the thalweg significantly decreased with time from the downstream section; subsequently, the thalweg recovered
296 a little after 2011. The deepening of the upstream was slower than that downstream, but the later recovery was more obvious
297 in the upstream area. The aspect ratio of the Zhuoshui River dramatically declined in the upstream part after construction of
298 the Jiji Dam; this change extended gradually to the downstream section with time. In the Dajia River, owing to the combined
299 effects of the upstream dam and the earthquake, channelization of the river started at both ends of the reach and then met in
300 the middle. The examples of these three rivers allow us to deduce the evolution of knickpoint retreat and transformation of the
301 river pattern under the influence of dams and/or uplift.

302 The river pattern of knickpoint retreat is illustrated in Fig. 12(b), and it was also observed in the Daan River. During the
303 knickpoint retreat, the tool effect caused the river to narrow dramatically. However, after the river had reached a new
304 equilibrium in a channelized pattern, the slope replacement resulted in a natural profile. The incision trend gradually slowed
305 during the adjustment, and sedimentation may commence downstream (dashed line in Fig. 12(b)). The profile evolved from a
306 concave curve to a graded profile (Chamberlin and Salisbury, 1904). In the case of the Daan River, the topography of the
307 upstream gorge was gradually swept away, and the river pattern may be slowly restored to the original braided plain.

308 Before construction of the Jiji Dam, the studied reach of the Zhoushui River was a broad braided river. The river armor
309 layer was lost due to sediment trapping by the dam. Under the influence of the tool effect, the flow path in front of the dam
310 gradually narrowed (Fig. 12(c)). The scouring boundary extended downstream-ward from the dam. Because of the immovable
311 knickpoint, the local slope at the dam toe became steeper, and the dam (acting as a non-erasable knickpoint) caused the river
312 profile and sediment transport to remain non-equilibrium state.

313 The reach downstream of the Shigang Dam on the Dajia River was simultaneously affected by coseismic uplift and the
314 incision of a deep path in the soft rock in front of the dam. The knickpoint caused by fault uplift retreated upward with time.
315 Although the uplift of the Dajia River was similar to that of the Daan River, the Shigang Dam (fixpoint) restricted knickpoint



316 retreatment in the Dajia River, and led to scouring downward from the dam site. Therefore, we saw the river narrowing at the
317 two ends of the affected reach, then progressively extending to the middle, as shown in Fig. 12(d). The knickpoint caused by
318 the earthquake was gradually removed, but the effect of the dam remains. Therefore, the restoration of the Daan River cannot
319 be seen in the Dajia River.

320 Overall, there are apparent differences in the morphological changes to rivers caused by natural and human factors. A
321 knickpoint formed by fault-induced riverbed uplift is a moving point: as the knickpoint moves, the riverbed evolves gradually
322 from an unstable state to an equilibrium. Topographic development is like the process of childhood to old age (Davis, 1899).
323 In contrast, a dam can be regarded as a fixpoint on the river. The flow from the spillway outlet hits the riverbed continuously,
324 resulting in a decline of the erosion base level; therefore, downward erosion commences from the toe of the dam. To summarize,
325 changes resulting from natural tectonic movements of a riverbed may achieve equilibrium with time, whereas imbalance
326 caused by anthropogenic structures may be enhanced with time. Therefore, we inferred a schematic diagram of longitudinal
327 profile development for the combined effects as shown in Fig. 13.

328 5. Conclusions

329 The Daan River, Zhoushui River, and Dajia River in central Taiwan exhibited changes in river morphology after
330 disturbance by earthquake uplift and dam obstruction during the past 20 years. The Daan River was affected by a thrust fault;
331 the Zhoushui River was influenced by dam obstruction; and the Dajia River was both fault- and dam-influenced. In the Daan
332 River, the greater slope accelerated the flow velocity and drove knickpoint retreat after removal of the armor layer, resulting
333 in the progress of slope replacement. However, the incision faded with time, sediment deposition commenced, and the river
334 showed potential for recovery. Because of sediment trapping by the Jiji Dam, the Zhoushui River has transformed from braided
335 to gorge. The channelization started from the dam and expanded downward, and the incision progress caused the local slope
336 at the toe to become steeper. Because the dam acts as an immovable knickpoint, the river's sediment equilibrium could not be
337 re-established. The Shigang Dam on the Dajia River also caused a downward incision. The incision from the toe of the dam
338 subsequently connected with the knickpoint retreat caused by headward erosion from downstream, forming a single,
339 meandering channel at the front of the dam.

340 Knickpoints resulting from fault-induced riverbed uplift are moving points: as the knickpoint moves, the riverbed
341 evolves gradually from an unstable state to an equilibrium state. In contrast, a dam, as a fixpoint on the river, causes continuous
342 degradation. When both effects exist on a reach, the impact of the knickpoint gradually fades away, but the results of the dam



343 on the river persist.

344 **Author contribution.**

345 The following contributions were made by the authors: HEC was involved in methods development, modeling, data
346 analysis, discussion, and paper preparation. YYC participated in data analysis, discussion, and paper preparation. CYC
347 conducted the field survey, collected and analyzed data. SCC contributed to the hypothesis, concept, research design,
348 conclusions, and paper preparation.

349 **Competing interests.**

350 The authors declare that they have no conflict of interest.

351 **Acknowledgements.**

352 The Ministry of Science and Technology, Taiwan, partially supports this research under grant No. 111-2625-M-005-001.
353 The authors would like to thank AFASI, MOST, and CSRSR/NCU for supplying satellite imagery data, and thank WRA for
354 supplying river measurement data.



355 References

- 356 Ahmed, M. F., Rogers, J. D., and Ismail, E. H.: Knickpoints along the upper Indus River, Pakistan: an exploratory survey of
357 geomorphic processes, *Swiss Journal of Geosciences*, 111, 191-204, doi:10.1007/s00015-017-0290-3, 2018.
- 358 Alonso, C. V., Bennett, S. J., and Stein, O. R.: Predicting head cut erosion and migration in concentrated flows typical of
359 upland areas, *Water Resources Research*, 38, 39-31-39-15, doi:10.1029/2001wr001173, 2002.
- 360 Bishop, P., Hoey, T. B., Jansen, J. D., and Artza, I. L.: Knickpoint recession rate and catchment area: the case of uplifted
361 rivers in Eastern Scotland, *Earth Surface Processes and Landforms*, 30, 767-778, doi:10.1002/esp.1191, 2005.
- 362 Braatne, J. H., Rood, S. B., Goater, L. A., and Blair, C. L.: Analyzing the impacts of dams on riparian ecosystems: a review
363 of research strategies and their relevance to the Snake River through Hells Canyon, *Environmental Management*, 41, 267-
364 281, doi:10.1007/s00267-007-9048-4, 2008.
- 365 Brandt, S. A.: Classification of geomorphological effects downstream of dams, *Catena*, 40, 375-401, doi:10.1016/S0341-
366 8162(00)00093-X, 2000.
- 367 Bressan, F., Papanicolaou, A. N., and Abban, B.: A model for knickpoint migration in first- and second-order streams,
368 *Geophysical Research Letters*, 41, 4987-4996, doi:10.1002/2014GL060823, 2014.
- 369 Chamberlin, T. C., and Salisbury, R. D.: *Geology: Geologic processes and their results*, H. Holt, 1904.
- 370 Choi, S. U., Yoon, B., and Woo, H.: Effects of dam-induced flow regime change on downstream river morphology and
371 vegetation cover in the Hwang River, Korea, *River Research and Applications*, 21, 315-325, doi:10.1002/rra.849, 2005.
- 372 Clark, M. K., Maheo, G., Saleeby, J., and Farley, K. A.: The non-equilibrium landscape of the southern Sierra Nevada ,
373 California, 5173, doi:10.1130/1052-5173(2005)15, 2014.
- 374 Cook, K. L., Turowski, J. M., and Hovius, N.: A demonstration of the importance of bedload transport for fluvial bedrock
375 erosion and knickpoint propagation, *Earth Surface Processes and Landforms*, 38, 683-695, doi:10.1002/esp.3313, 2013.
- 376 Cook, K. L., Turowski, J. M., and Hovius, N.: River gorge eradication by downstream sweep erosion, *Nature Geoscience*, 7,
377 682-686, doi:10.1038/ngeo2224, 2014.
- 378 Crosby, B. T., and Whipple, K. X.: Knickpoint initiation and distribution within fluvial networks: 236 waterfalls in the
379 Waipaoa River, North Island, New Zealand, *Geomorphology*, 82, 16-38, doi:10.1016/j.geomorph.2005.08.023, 2006.
- 380 Davis, W. M.: *Rivers and valleys of Pennsylvania*, Geographical essays by William Morris Davis, 413-513, 1889.
- 381 Engelund, F.: Instability of erodible beds, *Journal of Fluid Mechanics*, 42, 225-244, doi:10.1017/S0022112070001210, 1970.
- 382 Gardner, T. W.: Experimental study of knickpoint and longitudinal profile evolution in cohesive, homogeneous material,
383 *Geological Society of America Bulletin*, 94, 664-672, 1983.
- 384 Graf, W. L.: Downstream hydrologic and geomorphic effects of large dams on American rivers, *Geomorphology*, 79, 336-
385 360, doi:10.1016/j.geomorph.2006.06.022, 2006.
- 386 Hayakawa, Y. S., Matsuta, N., and Matsukura, Y.: Rapid recession of fault-scarp waterfalls: Six-year changes following the
387 921 Chi-Chi Earthquake in Taiwan, *Chikei/Transactions, Japanese Geomorphological Union*, 30, 1-13, 2009.
- 388 Heijnen, M. S., Clare, M. A., Cartigny, M. J. B., Talling, P. J., Hage, S., Lintern, D. G., Stacey, C., Parsons, D. R., Simmons,
389 S. M., Chen, Y., Sumner, E. J., Dix, J. K., and Hughes Clarke, J. E.: Rapidly-migrating and internally-generated knickpoints
390 can control submarine channel evolution, *Nature Communications*, 11, 3129-3129, doi:10.1038/s41467-020-16861-x, 2020.
- 391 Holland, W. N., and Pickup, G.: Flume study of knickpoint development in stratified sediment, *Geological Society of
392 America Bulletin*, 87, 76-82, doi:10.1130/0016-7606(1976)87<76:FSOKDI>2.0.CO;2, 1976.
- 393 Horn, J. D., Joeckel, R. M., and Fielding, C. R.: Progressive abandonment and planform changes of the central Platte River
394 in Nebraska, central USA, over historical timeframes, *Geomorphology*, 139, 372-383, doi:10.1016/j.geomorph.2011.11.003,
395 2012.



- 396 Howard, A. D., Dietrich, W. E., and Seidl, M. A.: Modeling fluvial erosion on regional to continental scales, *Journal of*
397 *Geophysical Research*, 99, doi:10.1029/94jb00744, 1994.
- 398 Huang, M.-W., Pan, Y.-W., and Liao, J.-J.: A case of rapid rock riverbed incision in a coseismic uplift reach and its
399 implications, *Geomorphology*, 184, 98-110, doi:10.1016/j.geomorph.2012.11.022, 2013.
- 400 Huang, M. W., Liao, J. J., Pan, Y. W., and Cheng, M. H.: Rapid channelization and incision into soft bedrock induced by
401 human activity - Implications from the Bachang River in Taiwan, *Engineering Geology*, 177, 10-24,
402 doi:10.1016/j.enggeo.2014.05.002, 2014.
- 403 Inbar, M.: EFFECT OF DAMS ON MOUNTAINOUS BEDROCK RIVERS, *Physical Geography*, 11, 305-319,
404 doi:10.1080/02723646.1990.10642409, 1990.
- 405 Kingsford, R. T.: Ecological impacts of dams, water diversions and river management on floodplain wetlands in Australia,
406 *Austral Ecology*, 25, 109-127, doi:10.1046/j.1442-9993.2000.01036.x, 2000.
- 407 Kong, D., Latrubesse, E. M., Miao, C., and Zhou, R.: Morphological response of the Lower Yellow River to the operation of
408 Xiaolangdi Dam, China, *Geomorphology*, 350, 106931-106931, doi:10.1016/j.geomorph.2019.106931, 2020.
- 409 Lee, J. C., Chu, H. T., Angelier, J., Chan, Y. C., Hu, J. C., Lu, C. Y., and Rau, R. J.: Geometry and structure of northern
410 surface ruptures of the 1999 Mw = 7.6 Chi-Chi Taiwan earthquake: Influence from inherited fold belt structures, *Journal of*
411 *Structural Geology*, 24, 173-192, doi:10.1016/S0191-8141(01)00056-6, 2002.
- 412 Lin, A., Ouchi, T., Chen, A., and Maruyama, T.: Co-seismic displacements, folding and shortening structures along the
413 Chelungpu surface rupture zone occurred during the 1999 Chi-Chi (Taiwan) earthquake, *Tectonophysics*, 330, 225-244,
414 doi:10.1016/S0040-1951(00)00230-4, 2001.
- 415 Liro, M.: Dam-induced base-level rise effects on the gravel-bed channel planform, *Catena*, 153, 143-156,
416 doi:10.1016/j.catena.2017.02.005, 2017.
- 417 Liro, M.: Dam reservoir backwater as a field-scale laboratory of human-induced changes in river biogeomorphology: A
418 review focused on gravel-bed rivers, *Science of the Total Environment*, 651, 2899-2912,
419 doi:10.1016/j.scitotenv.2018.10.138, 2019.
- 420 Lyell Sir, C., and Deshayes, G. P.: Principles of geology; being an attempt to explain the former changes of the earth's
421 surface, by reference to causes now in operation, J. Murray, London, 1830.
- 422 Magilligan, F. J., and Nislow, K. H.: Changes in hydrologic regime by dams, *Geomorphology*, 71, 61-78,
423 doi:10.1016/j.geomorph.2004.08.017, 2005.
- 424 Merritts, D., and Vincent, K. R.: Geomorphic response of coastal streams to low, intermediate, and high rates of uplift,
425 Medocino triple junction region, northern California, *GSA Bulletin*, 101, 1373-1388, doi:10.1130/0016-
426 7606(1989)101<1373:GROCST>2.3.CO;2, 1989.
- 427 Miodrag, S., and M, H. F.: 2-D Bed Evolution in Natural Watercourses—New Simulation Approach, *Journal of Waterway,*
428 *Port, Coastal, and Ocean Engineering*, 116, 425-443, doi:10.1061/(ASCE)0733-950X(1990)116:4(425), 1990.
- 429 Nelson, N. C., Erwin, S. O., and Schmidt, J. C.: Spatial and temporal patterns in channel change on the Snake River
430 downstream from Jackson Lake dam, Wyoming, *Geomorphology*, 200, 132-142, doi:10.1016/j.geomorph.2013.03.019,
431 2013.
- 432 Olsen, N. R. B.: Two-dimensional numerical modelling of flushing processes in water reservoirs, *Journal of Hydraulic*
433 *Research*, 37, 3-16, doi:10.1080/00221689909498529, 1999.
- 434 Ota, Y., Chen, Y.-G., and Chen, W.-S.: Review of paleoseismological and active fault studies in Taiwan in the light of the
435 Chichi earthquake of September 21, 1999, *Tectonophysics*, 408, 63-77, doi:10.1016/j.tecto.2005.05.040, 2005.



- 436 Parker, G., and Izumi, N.: Purely erosional cyclic and solitary steps created by flow over a cohesive bed, *Journal of Fluid*
437 *Mechanics*, 419, 203-238, doi:10.1017/S0022112000001403, 2000.
- 438 Petts, G. E., and Gurnell, A. M.: Dams and geomorphology: research progress and future directions, *Geomorphology*, 71,
439 27-47, doi:10.1016/j.geomorph.2004.02.015, 2005.
- 440 Seidl, M. A., and Dietrich, W. E.: The problem of channel erosion into bedrock, *Functional geomorphology*, 101-124, 1992.
- 441 Shafroth, P. B., Perry, L. G., Rose, C. A., and Braatne, J. H.: Effects of dams and geomorphic context on riparian forests of
442 the Elwha River, Washington, *Ecosphere*, 7, e01621-e01621, doi:10.1002/ecs2.1621, 2016.
- 443 Slowik, M., Dezső, J., Marciniak, A., Tóth, G., and Kovács, J.: Evolution of river planforms downstream of dams: Effect of
444 dam construction or earlier human-induced changes?, *Earth Surface Processes and Landforms*, 43, 2045-2063,
445 doi:10.1002/esp.4371, 2018.
- 446 Surian, N., and Rinaldi, M.: Morphological response to river engineering and management in alluvial channels in Italy,
447 *Geomorphology*, 50, 307-326, doi:10.1016/S0169-555X(02)00219-2, 2003.
- 448 Tomkin, J. H., Brandon, M. T., Pazzaglia, F. J., Barbour, J. R., and Willett, S. D.: Quantitative testing of bedrock incision
449 models for the Clearwater River, NW Washington State, *Journal of Geophysical Research: Solid Earth*, 108,
450 doi:10.1029/2001jb000862, 2003.
- 451 Whipple, K. X., and Tucker, G. E.: Dynamics of the stream-power river incision model: Implications for height limits of
452 mountain ranges, landscape response timescales, and research needs, *Journal of Geophysical Research: Solid Earth*, 104,
453 17661-17674, doi:10.1029/1999jb900120, 1999.
- 454 Whipple, K. X.: Fluvial landscape response time: how plausible is steady-state denudation?, *American Journal of Science*,
455 301, 313-325, doi:10.2475/ajs.301.4-5.313, 2001.
- 456 Whipple, K. X., and Tucker, G. E.: Implications of sediment-flux-dependent river incision models for landscape evolution,
457 *Journal of Geophysical Research: Solid Earth*, 107, ETG 3-1-ETG 3-20, doi.org/10.1029/2000JB000044, 2002.
- 458 Whipple, K. X.: BEDROCK RIVERS AND THE GEOMORPHOLOGY OF ACTIVE OROGENS, *Annual Review of Earth*
459 *and Planetary Sciences*, 32, 151-185, doi:10.1146/annurev.earth.32.101802.120356, 2004.
- 460 Williams, G. P., and Wolman, M. G.: Downstream effects of dams on alluvial rivers, 1286, 1984.
- 461 Zhou, M., Xia, J., Deng, S., Lu, J., and Lin, F.: Channel adjustments in a gravel-sand bed reach owing to upstream damming,
462 *Global and Planetary Change*, 170, 213-220, doi:10.1016/j.gloplacha.2018.08.014, 2018.

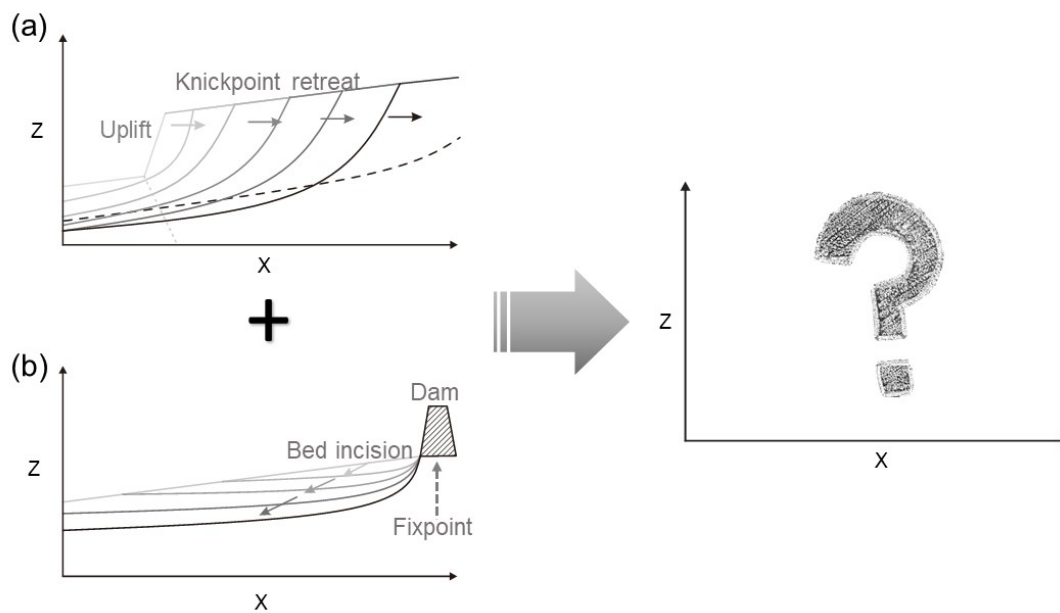


463

Table 1 Characteristics of the studied reaches of the Daan, Zhuoshui, and Dajia rivers

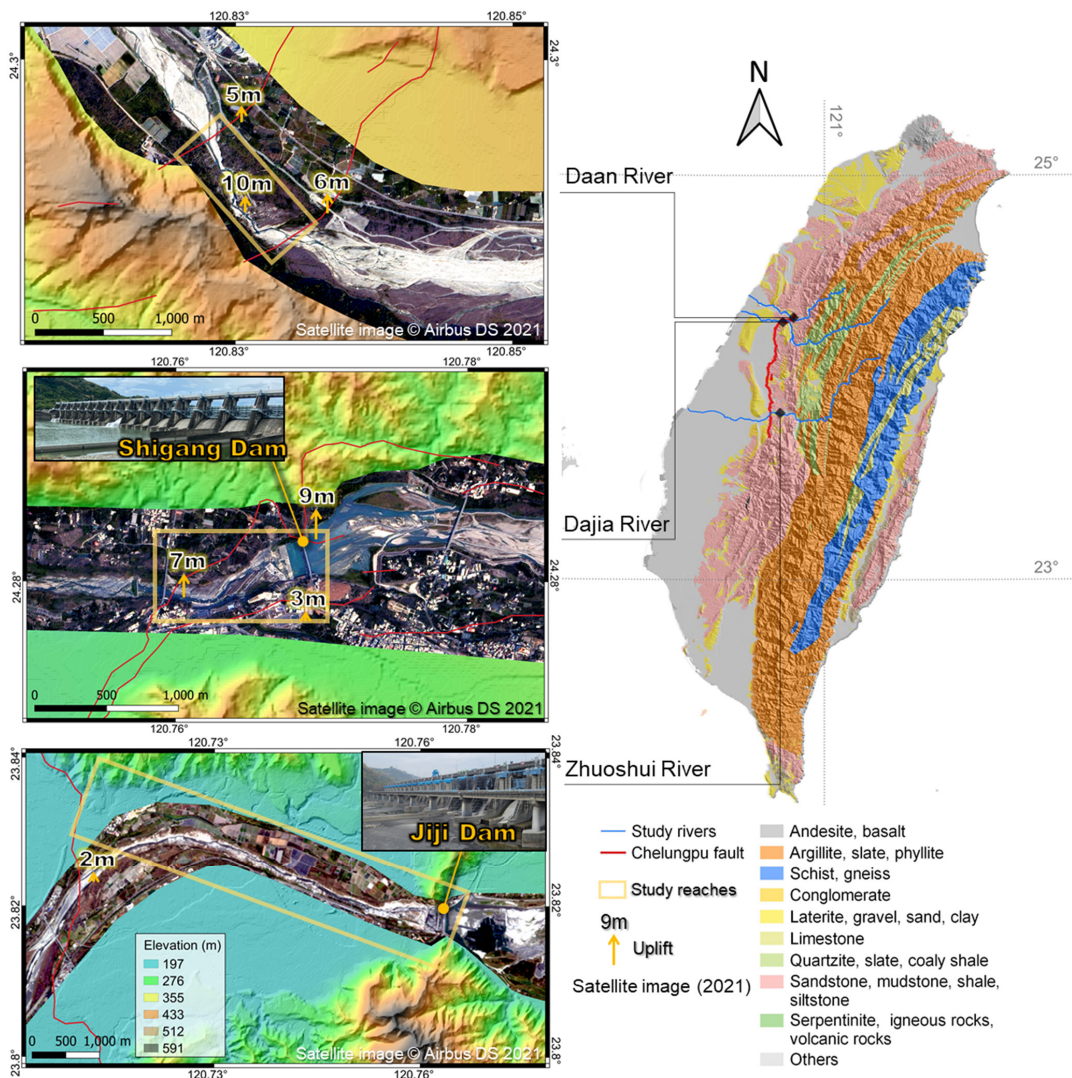
River	Time interval	Section	Bed Change		Channel Widening		Knickpoint retreat		C (m yr ⁻¹)	
			(m)	(m yr ⁻¹)	(m)	(m yr ⁻¹)	(m)	(m yr ⁻¹)		
Daan	2000–2004	a	-0.60	-0.15	-103.77	-25.94	85	21.25	22	
		b	-1.76	-0.44	47.50	11.88				
	2004–2007	a	-16.67	-5.56	-316.50	-105.50	422	140.67		
		b	-6.20	-2.07	-269.82	-89.94				
	2007–2011	a	2.06	0.52	19.30	4.83	412	103.00		
		b	-7.11	-1.78	-64.19	-16.05				
	2011–2016	a	-0.45	-0.09	31.19	6.24	--	--		
		b	-0.84	-0.17	41.27	8.25				
	Zhuoshui	1998–2008	c	-0.46	-0.05	-96.22	-9.62	--		--
			d	-2.24	-0.22	-130.41	-13.04			
e			-11.59	-1.16	-246.32	-24.63				
2008–2012		c	-5.44	-1.36	-258.44	-64.61	--	--		
		d	-2.77	-0.69	18.43	4.61				
		e	3.00	0.75	5.22	1.31				
2012–2015		c	-4.46	-1.49	-171.56	-57.19	--	--		
		d	-6.65	-2.22	-133.24	-44.41				
		e	-4.94	-1.65	-73.11	-24.37				
2015–2018		c	-0.84	-0.28	13.57	4.52	--	--		
		d	-0.86	-0.29	1.31	0.44				
		e	-3.03	-1.01	8.70	2.90				
Dajia		2000–2005	f	-2.39	-0.48	-14.12	-2.82	40	8.00	7.5
			g	-2.02	-0.40	-116.44	-23.29			
		2005–2008	f	-2.57	-0.86	-39.90	-13.30	186	62.00	
	g		-7.50	-2.50	-142.97	-47.66				
	2008–2014	f	-1.33	-0.22	12.28	2.05	--	--		
		g	-0.38	-0.06	2.21	0.37				
	2010–2014	h	-4.20	-1.05	-25.45	-6.36	219	24.33		
	2014–2017	f	-1.39	-0.46	-10.44	-3.48				
		g	-3.32	-1.11	8.84	2.95				
		h	-5.27	-1.76	-20.63	-6.88				

464



465

466 **Figure 1: Schematic diagrams of longitudinal profile development for (a) fault scarp's knickpoint, (b) dam's fixpoint,**
467 **and (c) How will the combined effects develop longitudinal profile?**

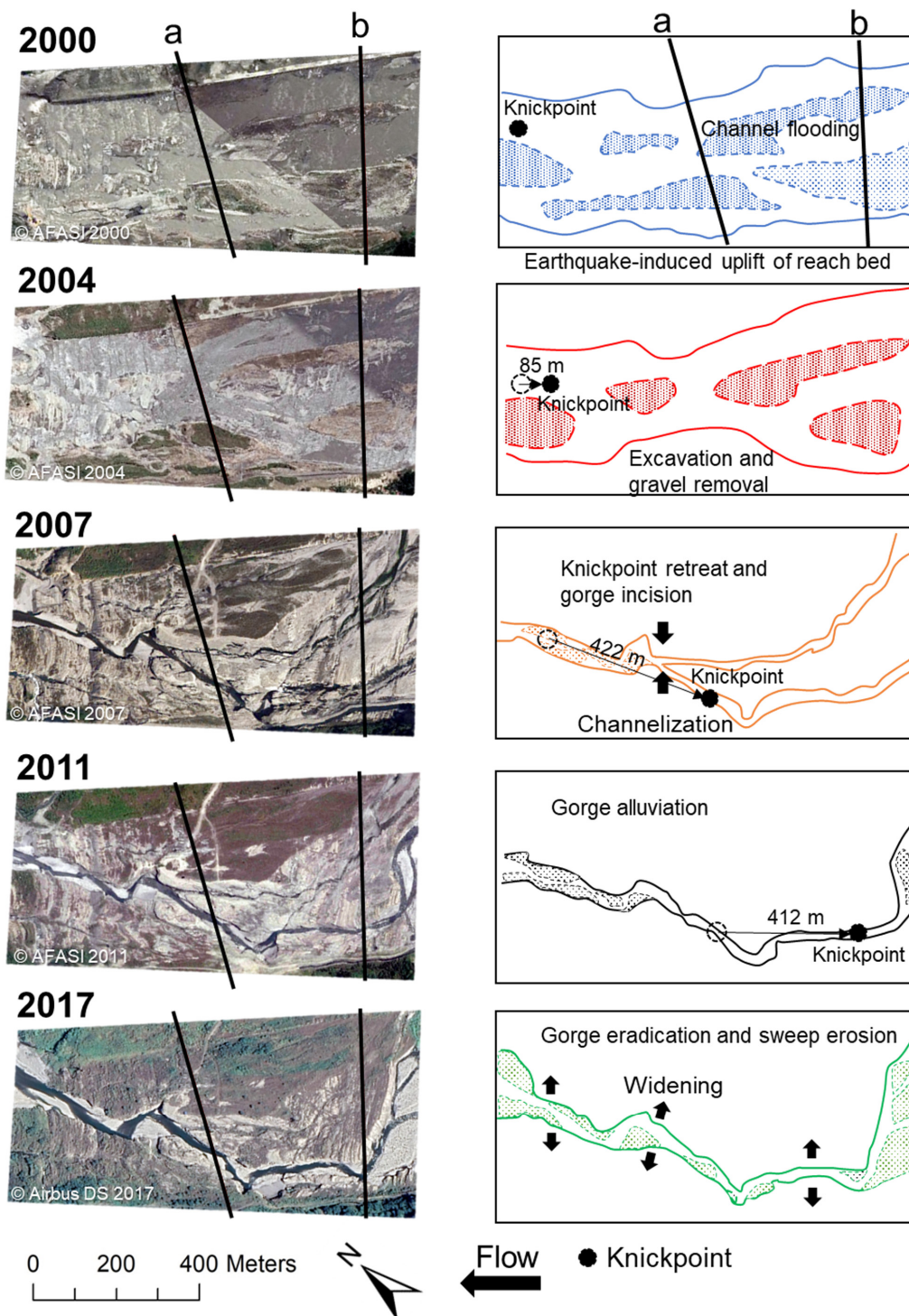


468

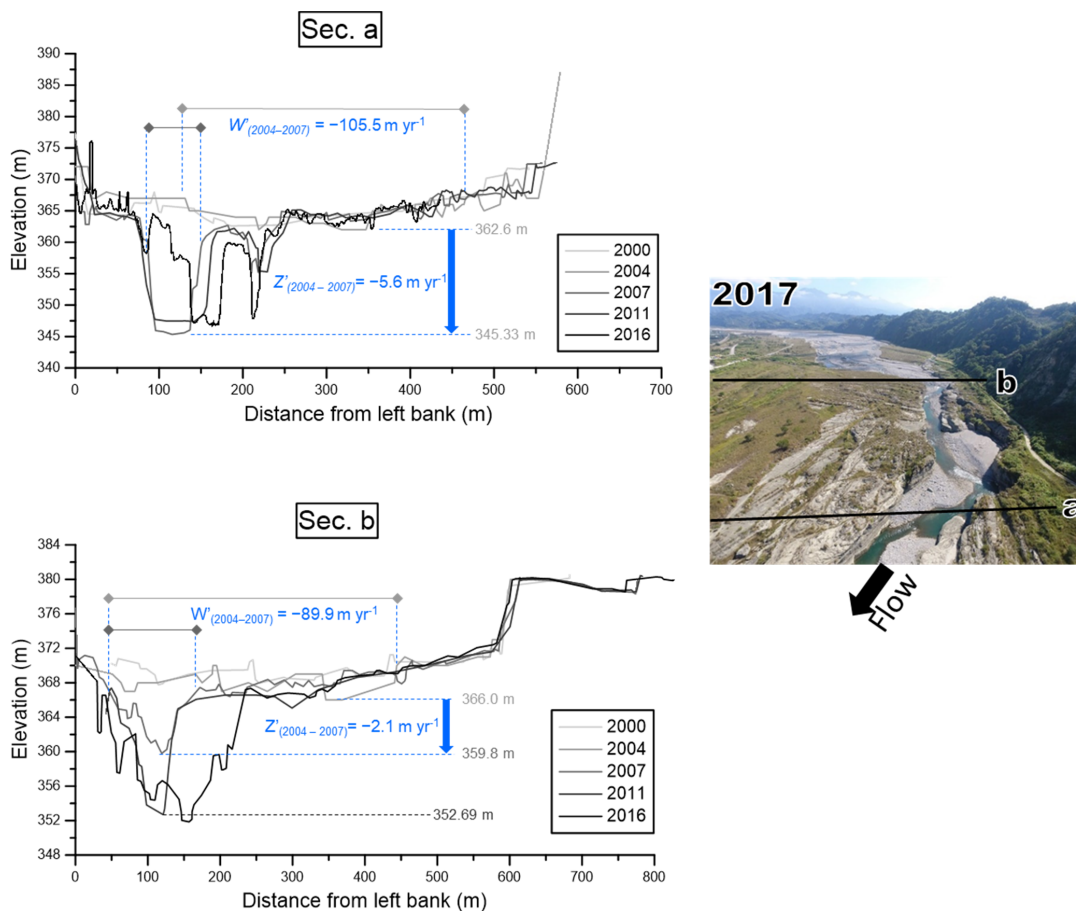
469

470

Figure 2: Locations of the Chelungpu Fault, the three studied rivers, and satellite images (from CSRSR/NCU) showing the studied reaches.



471
 472 **Figure 3: Orthographic images (2000–2011), satellite image (2017) and flow paths of the studied reach of the Daan**
 473 **River from 2000 to 2017.**



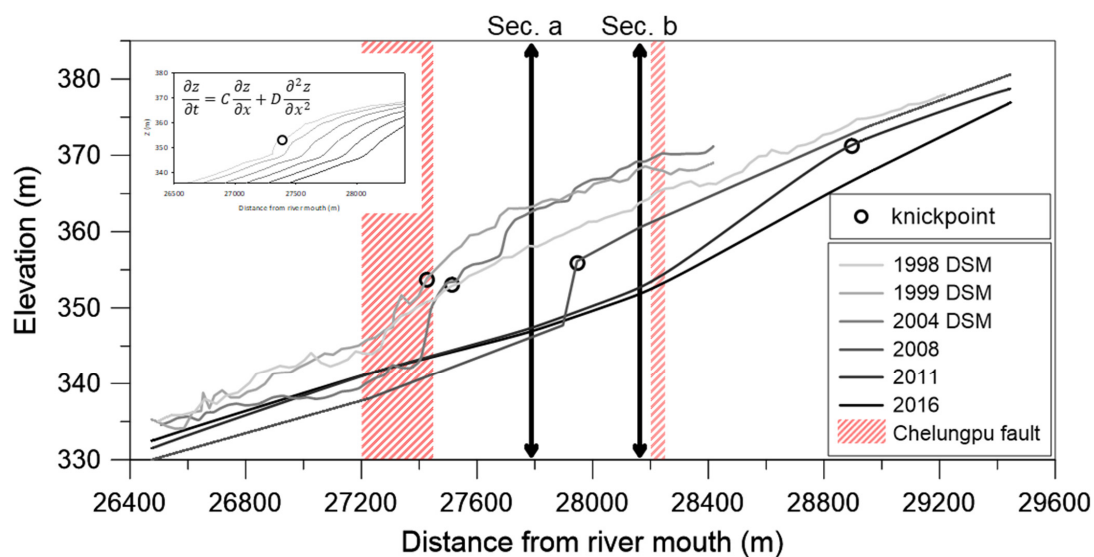
474

475 **Figure 4: Cross-sections a and b of the Daan River from 2000 to 2016 (from WRA).**

476



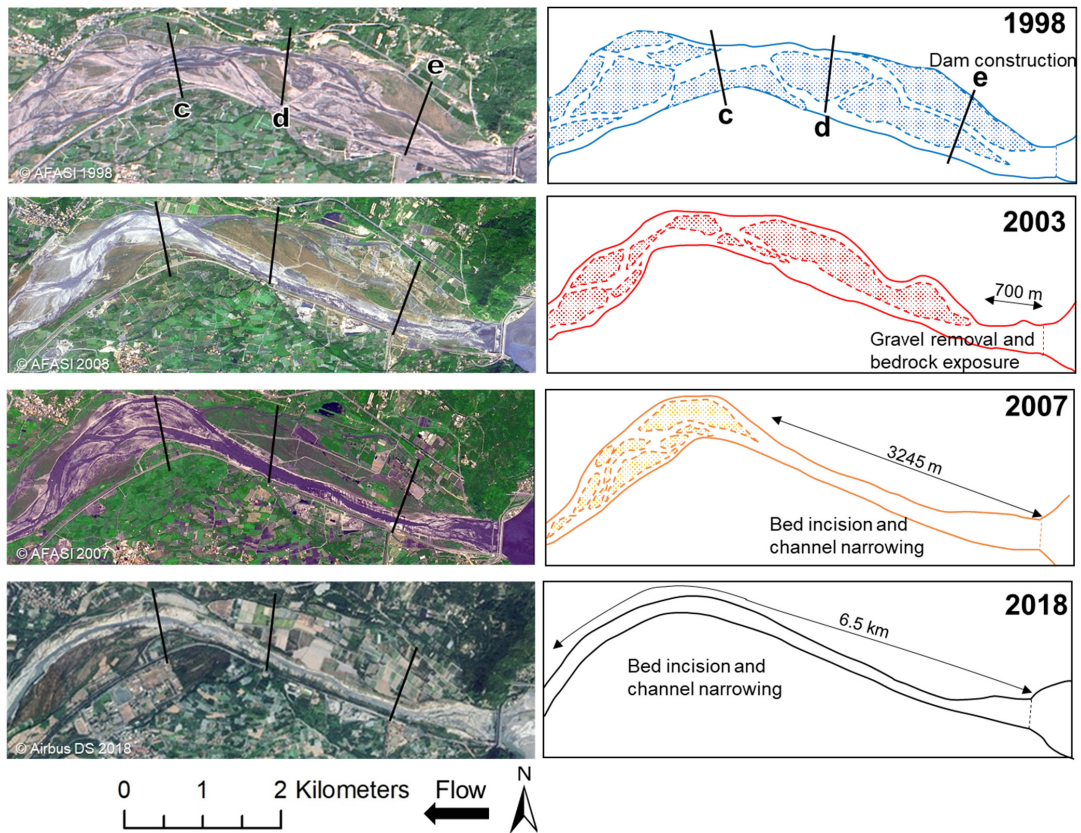
477



478

479 Figure 5: Longitudinal profiles of the studied reach of the Daan River from 2000 to 2016. Profiles for 1998–2008 are
480 from Cook et al. (2013), and 2011–2016 are from WRA. Data between 1998 and 2004 are derived from aerial photograph
481 generated Digital Surface Models (DSMs). Knickpoint retreats are simulated using the advective-diffusive model at the
482 top left.

483

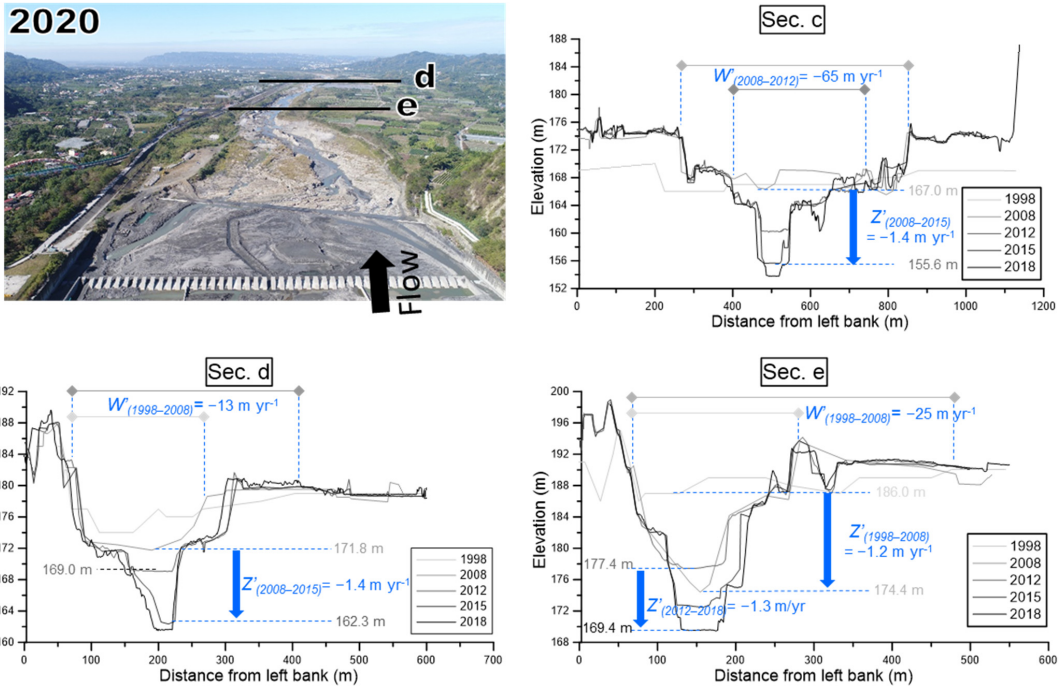


484

485 **Figure 6: Orthographic images (1998–2007), satellite image (2018), and flow paths of the studied reach of the Zhuoshui**

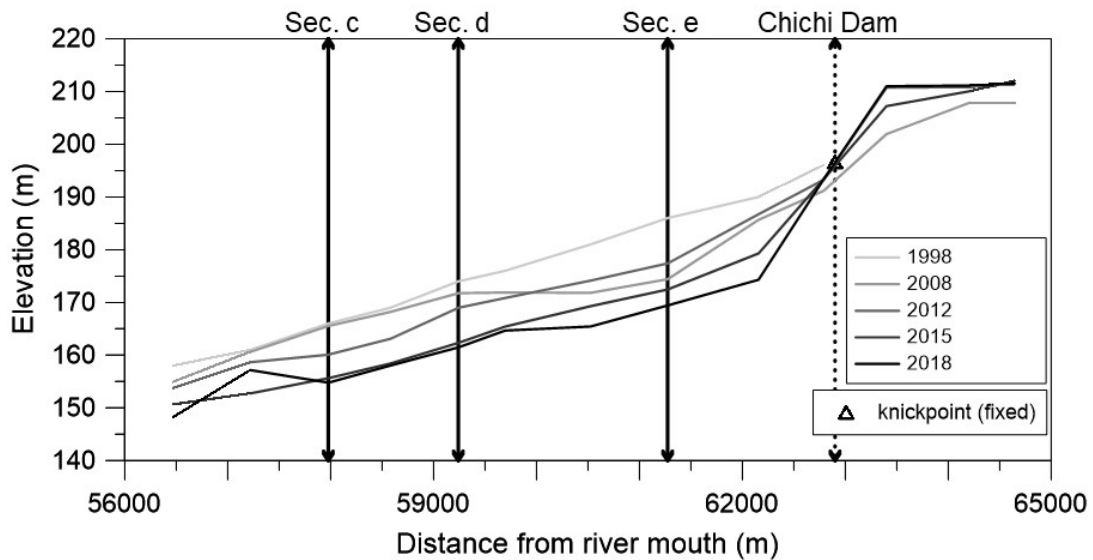
486 **River from 1998 to 2018.**

487



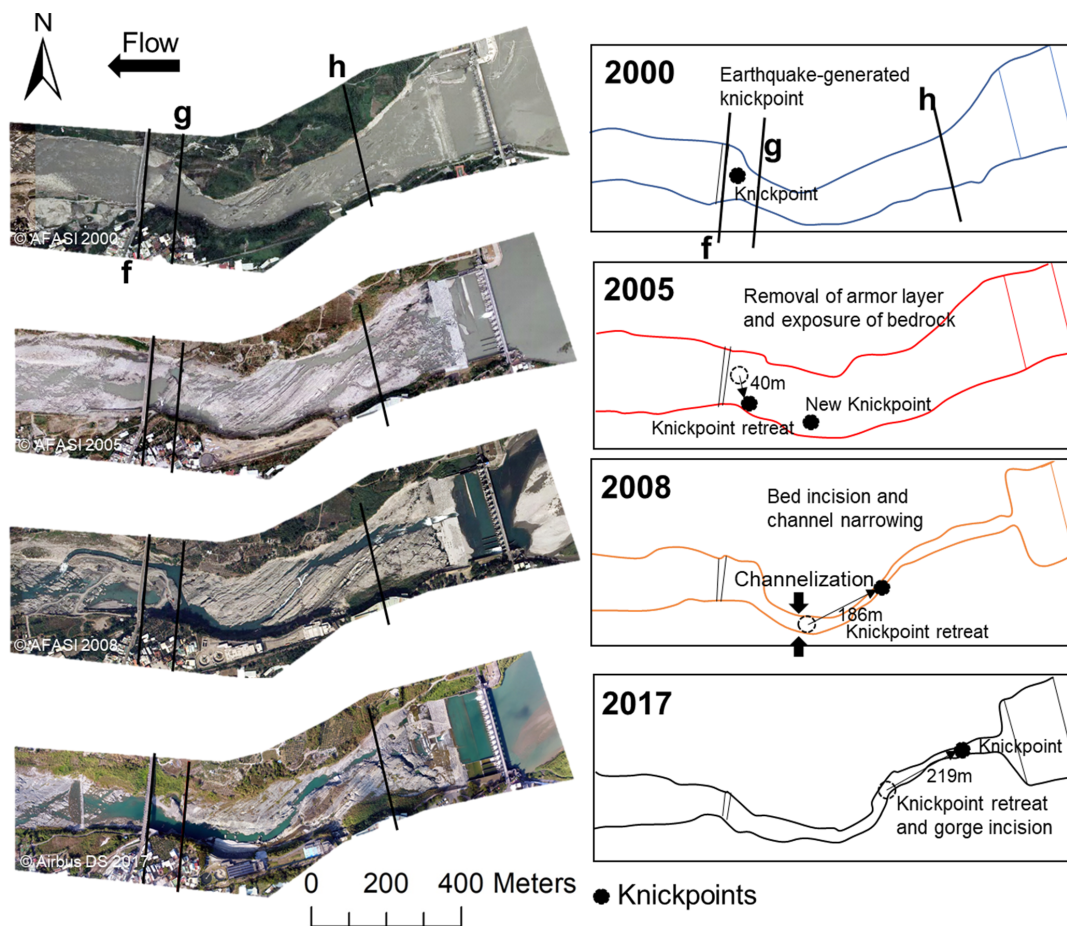
488
 489

Figure 7: Profiles of cross-sections c, d, and e of the Zhuoshui River from 1998 to 2018 (from WRA).

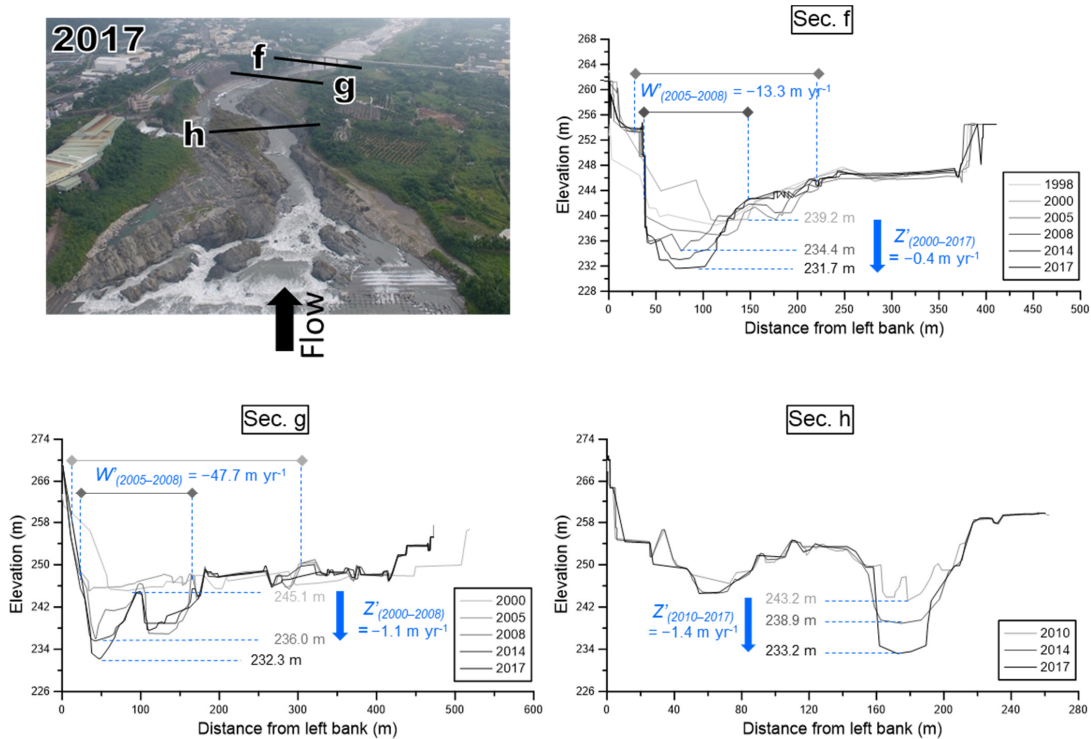


490
 491

Figure 8: Longitudinal profiles of the studied reach of the Zhuoshui River from 1998 to 2018 (from WRA).

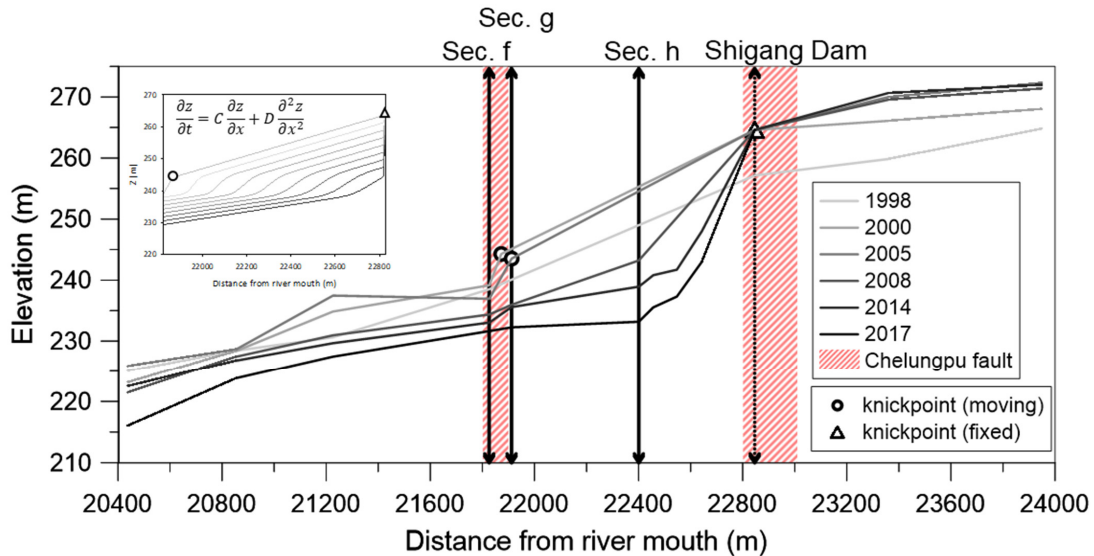


492
493 **Figure 9: Orthographic images (2000–2008), satellite image (2017), and flow paths of the Dajia**
494 **River from 2000 to 2017.**



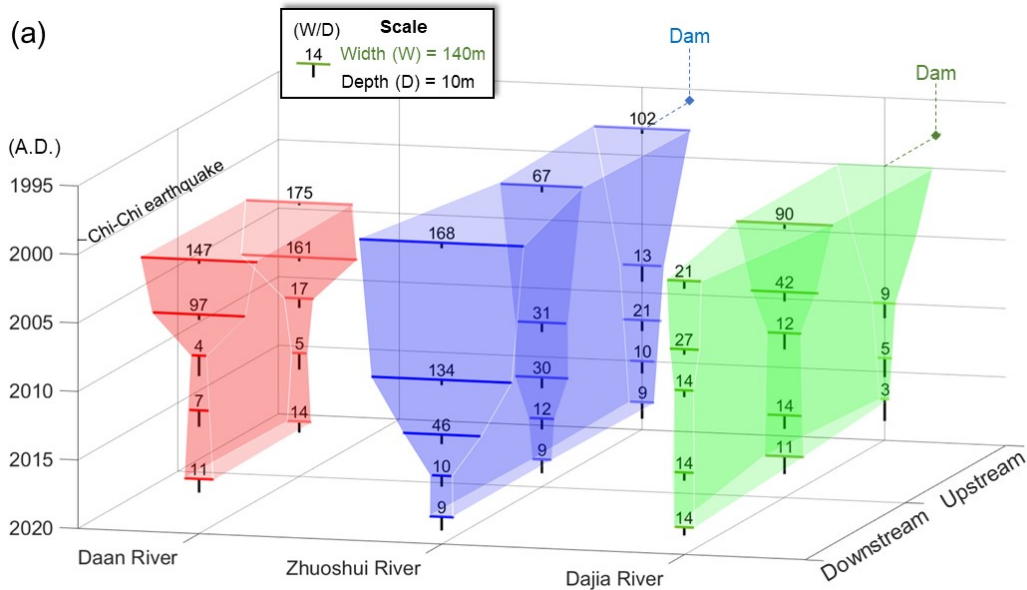
495
 496

Figure 10: Cross-sections f, g, and h of the Dajia River from 2000 to 2017 (from WRA).

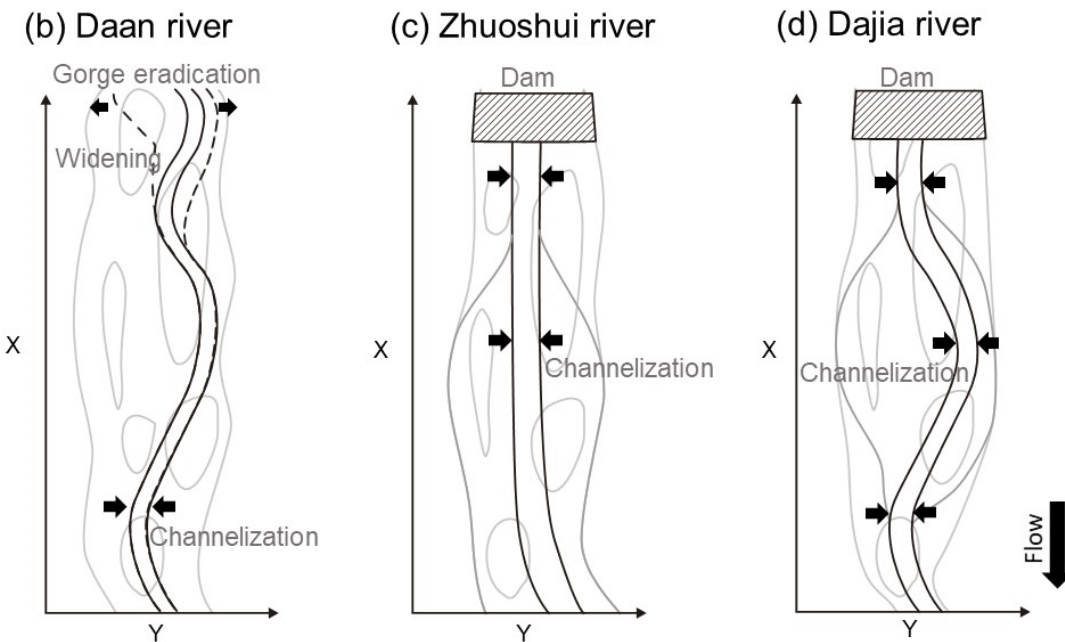


497
 498
 499

Figure 11: Longitudinal profiles of the studied reach of the Dajia River from 1998 to 2017 (from WRA). Knickpoint retreats are simulated using the advective-diffusive model at the top left.

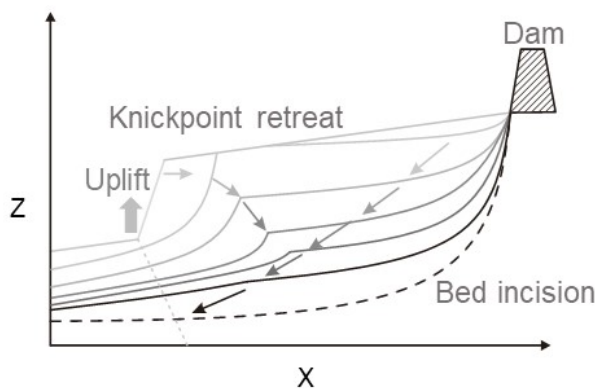


500



501

502 Figure 12: (a) Channel width (W), depth (D), and aspect ratio (W/D) of the studied reaches of the three rivers. The
 503 aspect ratio was defined as the ratio of the bankfull width to the depth of the bankfull channel. The vertical axis shows
 504 the time from 1995 downward to 2020, the horizontal axis shows the rivers, and the normal axis shows the sections
 505 from downstream to upstream. Schematic diagrams of knickpoint retreat and river pattern development for (b)
 506 coseismic uplift, (c) dam obstruction, and (d) dam obstruction and coseismic uplift.



507

508 **Figure 13: A Schematic diagram of longitudinal profile development for the combined effects from dam construction**

509 **and coseismic uplift.**

510

511